Influence of Sr substitution on the structure, charge distribution, and critical temperature of $Y(Ba_{1-x}Sr_x)_2Cu_4O_8$ single crystals

J. Karpinski,[1,*] S. M. Kazakov,[1] M. Angst,[1] A. Mironov,[2] M. Mali,[3] and J. Roos[3]
[1]*Solid State Physics Laboratory, ETH 8093 Zürich, Switzerland*
[2]*Chemical Department, Moscow State University, Moscow, Russia*
[3]*Physik Institut, Universität Zürich, 8057 Zürich, Switzerland*
(Received 29 January 2001; published 14 August 2001)

We have investigated the influence of substitution of Sr for Ba on the structure, charge distribution, and T_c in the $YBa_2Cu_4O_8$ (Y124) compound. Bond valence sum and nuclear quadrupole resonance investigations show that the substitution of Sr causes a redistribution of charge in the structure. The number of holes located in plane copper (Cu2) and apical oxygen (O1) increases, hence the number of holes in chain copper (Cu1) and plane oxygen (O2 and O3) decreases. A redistribution of holes from Cu1 to O1 and from O2 and O3 to Cu2 takes place. The literature data for Y123 and the hydrostatic pressure effect on both Y124 and Y123 compounds show that oxygen doping in Y123 and the pressure effect in Y124 increase the hole number equally on copper and oxygen. Therefore, although the number of holes on copper Cu2 in the CuO_2 planes increases with Sr doping in both Y124 and Y123, T_c does not rise as much as expected from the amount of charge transferred to Cu2, because of their distribution in the CuO_2 planes.

DOI: 10.1103/PhysRevB.64.094518 PACS number(s): 74.72.Bk, 61.10.Nz

I. INTRODUCTION

The family of $Y_2Ba_4Cu_nO_{2n+x}$ superconductors consists of three compounds for $n=6$, 7, and 8. The third member of the family ($n=8$) $YBa_2Cu_4O_8$ (Y124) contains a double CuO_2 chain instead of a single chain as in Y123.[1] Figure 1 shows the structure of Y124 and Y123. The second compound ($n=7$) $Y_2Ba_4Cu_7O_{14+x}$ (Y247) contains alternating double and single chains,[2] which make its structure exceptional because the two CuO_2 superconducting planes are structurally nonequivalent. The Y124 compound is also unusual among all superconducting cuprates due to the fact that the oxygen content is fixed to eight in the formula unit. This is caused by the higher coordination number of oxygen in double chains than in single chains. Each oxygen atom has three neighboring copper atoms instead of two in Y123. Y124 is a stoichiometric, intrinsically underdoped compound. Therefore it is possible to investigate superconducting parameters as a function of substitutions without any danger of an influence of oxygen nonhomogeneity. This is especially important for investigations on small single crystals, where a determination of the oxygen content is very difficult. As we have shown in the past, differences in the oxygen content have strong influence on such parameters like γ or the irreversibility field $H_{\rm irr}$.[3] Our investigations of superconducting parameters performed on Y124 single crystals show a higher anisotropy than Y123, $\gamma=12$ for unsubstituted crystals,[4] in line with the underdoped nature of Y124. Investigations on single crystals are crucial for the determination of superconducting parameters γ, penetration depth λ, coherence length ξ, $H_{\rm irr}$ and the *H-T* phase diagram. Powder samples usually contain foreign phases, and influence of granularity effects on magnetic properties is unavoidable.[5] Due to the high anisotropy of superconducting parameters it is very difficult to measure intrinsic parameters of these compounds on such samples.

In the present work we investigate the influence of substitution of Sr for Ba in the Y124 compound on the structure, charge distribution, and critical temperature. The Sr atom (ionic radius $r_1=1.36$ Å) is smaller than the Ba radius ($r_1=1.52$ Å),[6] therefore one can expect an effect of chemical pressure on the structure. Unfortunately, the situation is more complex than expected. The first high-T_c superconductor, $La_{2-x}Ba_xCuO_4$ exhibits a high positive pressure effect on T_c.[7] In fact, a partial substitution of Sr for Ba led to an increase of T_c from 28 to 36 K.[8] Substitution of Sr for Ba in Y123 and Hg-based superconductors shows a negative effect on T_c, although the pressure effect on T_c is positive in both compounds.[9,10] This indicates that chemical pressure is not equivalent to the application of mechanical pressure on the material. Pressure causes a charge transfer from the chains to the planes.[11,13] However, also the hole distribution between Cu and O sites of CuO_2 planes is important for T_c, as suggested by several authors using nuclear quadrupole resonance (NQR),[12,13] near-edge x-ray-absorption fine structure,[14] as well as bond-valence sum (BVS) analysis.[15] We will discuss this below.

Y124 shows a very high positive pressure effect on T_c, $dT_c/dp=5$ K/GPa.[16] A comparison of the effects of chemical and mechanical pressure on Y124 and Y123 is presented. Y124 is one of the few compounds where Sr substitution increases T_c, although structural changes are similar to those in Y123. Investigations of the substitution of Sr for Ba in Y124 and Y247 have been performed in the past on polycrystalline samples,[17–19] which made investigation of intrinsic physical parameters difficult. In our work structural investigations are performed on single crystals, which are later used for investigation of superconducting parameters γ, λ, ξ, and $H_{\rm irr}$,[20] while NQR was performed on polycrystalline samples because of the required larger mass of the sample.

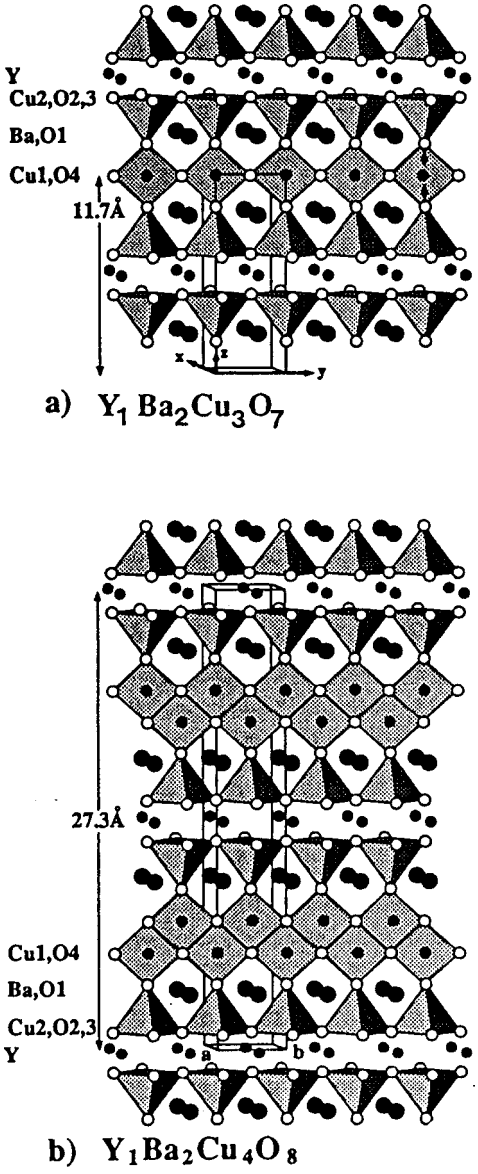

FIG. 1. Structure of (a) $YBa_2Cu_3O_{7-\delta}$ and (b)$YBa_2Cu_4O_8$.

II. EXPERIMENT

A. Crystal growth

For the growth of Y124 and Y124 Sr crystals we used a nonstoichiometric flux technique, a BaO-CuO eutectic mixture has been used as a flux. The total composition of the samples corresponds to a metal ratio Y:Ba:Cu equal to 1:15:30. In the case of Sr-substituted crystals, a part of Ba was substituted with Sr. Several Ba:Sr ratios were used: 15:1, 8:1, 5:1, 4:1, 3:1. As a precursor, we used mixtures of Y123 (99.9% Aldrich), BaO_2, SrO, and CuO (99.99%, Aldrich). Pellets of starting materials with a total mass of about 20 g were placed into the crucible and subjected to a high-pressure oxygen treatment. According to the phase diagram[21] for the growth of Y124 crystals, high oxygen pressure above 500 bar is necessary. The high-pressure system consists of a double-chamber vessel. The internal chamber is made of Al_2O_3 and contains oxygen at high pressure. The furnace works in an argon atmosphere at exactly the same pressure as the oxygen. This apparatus can work up to $P_{O_2}<3000$ bar at $T<1300\,^{\circ}$C. Typically we grow crystals at $P_{O_2}=900$ bar. The melting temperature of the flux at this pressure is about 1100 °C. A crucial problem is the choice of the crucible material. All known ceramic materials react with the molten Ba-Cu-O flux. After many experiments with Al_2O_3, ZrO_2, $BaZrO_3$, and Y_2O_3 crucibles the best results were obtained with Y_2O_3 ones. These crucibles react also with the molten flux forming the Y_2BaCuO_5 phase, but do not dope crystals with foreign elements. The typical temperature run consists of (1) heating up to 1000 °C, (2) dwelling for half an hour, (3) heating up to 1100–1120 °C, (4) dwelling for 1–3 h, (5) slowly cooling down to 1080–1090 °C with a rate of 1–2 °C/h, and (6) cooling down to room temperature with a rate of 5°/min. Crystals of a size up to several mm and weight up to 3 mg have been obtained.[21]

Synthesis of polycrystalline Y124:Sr samples has been done at high oxygen pressure. As a precursor we used a mixture of Y123:Sr (prepared at $P_{O_2}=1$ bar) and CuO (99.99%, Aldrich). Pellets of the starting materials, with a total mass of about 3 g, were placed into the crucible and subjected to the high-pressure oxygen ($P_{O_2}=450$ bar), high-temperature ($T=1000\,^{\circ}$C) treatment for 40 h.

B. Structural investigations

Several crystals with different Sr content from different crystal-growth experiments were chosen for single-crystal x-ray analysis. The description of the x-ray single-crystal experiments is given in Table I.

Cell parameters for each crystal were obtained from one and the same set of 23 reflections, the positions of which were determined using standard SET4 procedure. θ and hkl ranges for all experiments were the same. Absorption correction was applied in each case according to the shape of each crystal. The total number of reflections was about 5000. Some reflections in each data set were excluded from refinement according to the following criteria. Reflections, whose intensity were determined with an attenuator (from 2 to 6 depending on a sample) were not used in refinement. Profiles of all reflections in each set were visually checked. Reflections that had only one component (either $K\alpha1$ or $K\alpha2$) were eliminated from refinement too as well as reflections that had no right profile (from 20 to 50 depending on the set). The last criteria deals with the number of equivalents. If the number of equivalent reflections were half (or lower) of the possible number of reflections, reflection was rejected. The total number of eliminated reflections did not exceed 10% of the totally observed for each crystal.

The structures were refined by JANA2000 program package.[22] Starting parameters were taken from Ref. 23. Each structure was refined with isotropic atomic-displacement parameters; then Ba content was refined for each case (Sr content was considered to be $1-x$, where x is Ba occupancy) and finally simultaneous refinement of occupancies and anisotropic displacement parameters was undertaken. Then the compositions of the crystals were corrected, absorption corrections were applied, and the refinements

TABLE I. Summary of crystallographic information for $Y(Ba_{1-x}Sr_x)_2Cu_4O_8$ phases.

Sr content x	0	0.11	0.16	0.31
Crystal system		Orthorhombic		
Space group		*Ammm*		
a (Å)	3.8402(2)	3.8299(2)	3.8232(2)	3.8086(1)
b (Å)	3.8702(3)	3.8676(2)	3.8644(2)	3.8601(2)
c (Å)	27.2283(30)	27.1707(20)	27.1387(20)	27.0588(24)
Z		2		
d_{calc}	6.118	6.062	6.043	5.967
Radiation/wavelenghth		Mo Kα/0.71073 Å		
θ range for parameters refinement		17.1–34.9		
Temperature K		293		
Crystal form		Plate		
Crystal size (mm)	0.39×0.11×0.03	0.26×0.12×0.02	0.28×0.13×0.02	0.34×0.15×0.065
Color		Black		
Diffractometer		CAD4, Graphit monochromator		
Scan mode		$\omega/1.33\theta$		
Absorption correction		Analytical (crystal shape)		
θ range (data collection)		2–50		
Range of h,k,l		$-1\rightarrow h\rightarrow 8.\ -8\rightarrow k\rightarrow 8.\ -58\rightarrow l\rightarrow 58$		
Exctinction×10^5	0.678(9)	0.474(6)	0.218(6)	0.153(5)
R_{int}	0.03	0.028	0.033	0.031
Refinement on		F		
R/R_w $[I>3\sigma(I)]$	0.014/0.019	0.015/0.019	0.016/0.018	0.020/0.026
Gof/wGof	0.97/2.68	1.01/2.61	0.78/2.38	2.82/3.75
No. of parameters	42	34	43	43
N_{ref}/N_{par}	24.21	28.79	22.72	22.35
$(\Delta/\sigma)_{max}$		0.0005		
Δr_{max} (e/Å^{-3})[a] positive/negative	1.06/2.02	1.44/2.19	1.01/1.42	1.45/1.53

[a]Maximal electron density for oxygen atoms ranging from 20.7 to 33.4 e/Å^{-3} depending on the structure and site.

were repeated. If necessary this procedure was repeated once more until changes in composition did not occur.

All cations in each structure were refined with anharmonic displacement parameters up to the fourth harmonic and probability density functions (PDF's) were calculated. In all structures Y, Cu1, and Cu2 sites showed large negative regions, and anharmonic refinement was rejected for these atoms. For three structures, negative regions at Ba-site PDF maps had negative values less than 1% of the maximal probability, and anharmonic displacement parameters were accepted. For the $YBa_{1.78}Sr_{0.22}Cu_4O_8$ crystal such negative regions were about 5–7 % of the highest probability value and cations in this structure were refined in anisotropic approximation of atomic displacement parameters. At the final stage Ba and Sr occupancies were refined independently. In all cases the total occupancy (Ba+Sr) of the Ba site was close (or below) to 1 within two standard deviations. Finally the total occupancy of that site was considered to be full and the sum of partial occupancies was constrained.

The refined atomic parameters are given in Table II; interatomic distances, selected bond angles, and separation of some atoms from the CuO_2 weighted plane are given in Table III. The detailed description of the structures will be given in a separate paper.

C. Nuclear quadrupole resonance

The frequency ν_Q of a NQR signal depends on the principal components V_{ii} of the electric-field gradient (EFG) tensor present at the nuclear site of the atom. For the two naturally occurring nuclear spin-$\frac{3}{2}$ copper isotopes ^{63}Cu and ^{65}Cu measured in our experiment, ν_Q is given by the expression

$$\nu_Q = \frac{eQV_{zz}}{2h}\sqrt{1+\tfrac{1}{3}\eta^2}.$$

Here, η is the asymmetry parameter defined as $\eta=(V_{xx}-V_{yy})/V_{zz}$, where $|V_{zz}|\geqslant|V_{yy}|\geqslant|V_{xx}|$ and eQ is the nuclear electric quadrupole moment.

The EFG tensor consists essentially of two contributions, one coming from the charge distribution of the surrounding ions in the crystal lattice (lattice contribution) and the other arising from the on-site electron distribution in the incompletely filled electronic shell of the Cu atom (valence contribution). Therefore, the EFG and hence ν_Q are very sensitive to the variations in the oxygen coordination, Cu-O bond length, and the electronic structure, and can thus deliver valuable information about the microscopic effects of ion substitutions, doping, lattice distortions, etc.

The NQR experiments were performed on the Cu nuclei in zero magnetic field by using a standard pulsed spectrom-

TABLE II. Refined atomic parameters of Sr-substituted 124 phases.

Sr content x	0	0.11	0.16	0.31
Refined composition	Ba_2	$Ba_{1.72}Sr_{0.22}$	$Ba_{1.68}Sr_{0.32}$	$Ba_{1.38}Sr_{0.62}$
EDX analysis	Ba_2	$Ba_{1.76}Sr_{0.24}$	$Ba_{1.68}Sr_{0.32}$	$Ba_{1.42}Sr_{0.58}$
U_{11}, Y/$\frac{1}{2},\frac{1}{2},0$)	0.004 79(6)	0.005 10(6)	0.005 71(7)	0.005 08(7)
U_{22}, Y	0.004 44(6)	0.004 58(6)	0.004 11(6)	0.004 49(6)
U_{33}, Y	0.005 84(6)	0.005 08(6)	0.006 68(6)	0.007 12(6)
$\frac{1}{2},\frac{1}{2}$ z, Ba	0.134 815(6)	0.134 936(3)	0.134 902(7)	0.134 036(7)
U_{11}, Ba	0.006 95(9)	0.007 69(3)	0.009 53(11)	0.008 08(11)
U_{22}, Ba	0.005 56(8)	0.006 06(3)	0.005 60(9)	0.006 28(11)
U_{33}, Ba	0.008 38(8)	0.009 10(3)	0.010 76(10)	0.012 05(12)
0, 0, z, Cu1	0.212 974(4)	0.212 926(6)	0.212 899(6)	0.212 846(7)
U_{11}, Cu1	0.012 09(7)	0.014 74(8)	0.016 74(9)	0.018 78(10)
U_{22}, Cu1	0.004 39(6)	0.004 36(6)	0.004 23(6)	0.004 71(7)
U_{33}, Cu1	0.004 83(5)	0.005 11(5)	0.005 81(5)	0.006 66(6)
0, 0, z, Cu2	0.061 535(6)	0.061 796(6)	0.061 985(6)	0.062 297(6)
U_{11}, Cu2	0.003 94(6)	0.004 20(5)	0.004 75(6)	0.004 45(6)
U_{22}, Cu2	0.003 57(5)	0.003 76(5)	0.003 23(6)	0.003 64(6)
U_{33}, Cu2	0.007 54(6)	0.007 87(6)	0.008 32(6)	0.008 48(6)
0, 0, z, O1	0.145 45(4)	0.145 23(4)	0.145 24(4)	0.144 87(4)
U_{11}, O1	0.012 7(4)	0.017 5(5)	0.020 5(5)	0.025 2(6)
U_{22}, O1	0.008 9(3)	0.012 7(4)	0.010 3(4)	0.012 8(4)
U_{33}, O1	0.006 3(3)	0.006 6(4)	0.006 9(3)	0.007 3(3)
$\frac{1}{2}$, 0, z, O2	0.052 31(4)	0.052 40(4)	0.052 58(4)	0.052 64(4)
U_{11}, O2	0.004 3(3)	0.004 4(3)	0.005 4(3)	0.004 5(3)
U_{22}, O2	0.006 5(3)	0.006 2(3)	0.006 3(3)	0.006 8(3)
U_{33}, O2	0.010 6(3)	0.012 0(4)	0.012 9(4)	0.013 5(4)
0, $\frac{1}{2}$, z, O3	0.052 37(4)	0.052 53(4)	0.052 72(4)	0.052 88(4)
U_{11}, O3	0.007 0(3)	0.007 7(4)	0.008 4(3)	0.008 4(4)
U_{22}, O3	0.004 6(3)	0.004 3(3)	0.003 4(3)	0.004 2(3)
U_{33}, O3	0.009 0(3)	0.009 6(3)	0.011 0(3)	0.011 4(3)
0, $\frac{1}{2}$, z, O4	0.217 96(4)	0.217 93(4)	0.217 81(4)	0.217 79(4)
U_{11}, O4	0.024 3(5)	0.027 5(6)	0.029 8(6)	0.032 9(7)
U_{22}, O4	0.006 4(3)	0.006 3(3)	0.005 8(3)	0.006 5(3)
U_{33}, O4	0.007 0(3)	0.007 3(3)	0.007 7(3)	0.008 0(3)

eter and employing the spin-echo technique. Scanning the spectrometer frequency in 100-kHz steps, the complex-valued spin-echo signals were measured in quadrature and afterwards integrated over time. By plotting the magnitude of the echo integral versus frequency we obtained in a point-wise fashion the NQR line.

III. RESULTS AND DISCUSSION

A. Determination of T_c

The transition temperature of the crystals was determined by superconducting quantum interference device magnetometry. The magnetization was measured as a function of temperature in an applied field of 1 Oe—both zero field and field cooled. Figure 2 shows zero-field-cooled magnetization curves of single crystals (a) and powder samples (b). The critical temperature T_c of Y124 samples with small Sr content ($x \approx 0.1$) is lower than unsubstituted ones; samples with higher Sr content ($x \geqslant 0.2$) have higher T_c than pure Y124. Both single crystals and powder samples show such an effect. Possible explanation can be the influence of disorder created by the substitution, which is competitive to the charge-transfer effect and can decrease T_c.[24] However, for single crystals these variations are more pronounced. Unsubstituted Y124 single crystal has an effective critical temperature $T_{c,\mathrm{eff}}=77.7$ K, which decreases by about 1.7 K after substitution of 12% Sr for Ba. After substitution of 30% Sr $T_{c,\mathrm{eff}}$ increases up to 80.5 K. The whole change is 4.5 K. For unsubstituted polycrystalline sample $T_{c,\mathrm{eff}}=80.5$, which decreases by about 0.7 K after substitution of 10% Sr. After substitution of 30% Sr $T_{c,\mathrm{eff}}$ increases up to 81.2 K. The whole change is 1.4 K, which is 31% of this for single crystals. The reason for this difference can be a different distribution of Sr in single crystals and powder. Single crystals have been grown from the melt at 1100 °C. In a melt one can expect homogeneous distribution of all components. Polycrystalline samples have been obtained at 1000 °C in a solid-state reaction. The diffusion of components in a solid state is

TABLE III. Interatomic distances, selected bond angles, and separation of atoms from CuO_2 weighted plane.

x, Sr content	0	0.11	0.16	0.31
Y-O2 Å×2	2.4028(6)	2.4014(6)	2.40200	2.3987(7)
Y-O3 Å×2	2.3917(6)	2.3883(6)	2.3877(7)	2.3820(7)
Ba-O1 Å×4	2.7414(7)	2.7358(8)	2.7325(9)	2.7246(8)
Ba-O2 Å×2	2.9650(8)	2.9612(8)	2.9537(10)	2.9469(9)
Ba-O3 Å×2	2.9540(8)	2.9462(8)	2.9375(10)	2.9250(8)
Ba-O4 Å×2	2.9686(8)	2.9584(8)	2.9524(10)	2.9415(9)
Cu1-O1 Å	1.8386(10)	1.8394(10)	1.8361(10)	1.8395(12)
Cu1-O4 Å	1.8805(10)	1.8787(10)	1.8805(11)	1.8770(11)
Cu1-O4 Å×2	1.9399(10)	1.9386(10)	1.9368(11)	1.9347(12)
Cu2-O1 Å	2.2848(10)	2.2669(10)	2.2595(10)	2.2342(10)
Cu2-O2 Å×2	1.9365(8)	1.9319(10)	1.9286(10)	1.9221(8)
Cu2-O3 Å×2	1.9511(8)	1.9501(10)	1.9485(10)	1.9468(8)
CuO_2 plane[a]-O2 Å	−0.245	−0.249	−0.249	−0.256
CuO_2 plane[a]-O3 Å	−0.243	−0.246	−0.246	−0.249
CuO_2 plane[a]-Cu2 Å	0.006	0.006	0.006	0.006
CuO_2 plane[a]-Cu2 Å	10.270	10.233	10.211	10.164
Next perovskite block				
CuO_2 plane[a]-Ba Å	2.002	1.993	1.985	1.971
Neighboring layer				
CuO_2 plane[a]-Ba Å	8.274	8.246	8.232	8.198
Next perovskite block				
CuO_2 plane[a]-Y Å	1.669	1.673	1.676	1.680
Cu2-O2-Cu2 (deg)	165.09	164.81	164.79	164.37
Cu2-O3-Cu2 (deg)	165.30	165.16	165.17	164.96

[a]Weighted CuO_2 plane.

much slower than in a melt. Therefore one can expect some nonhomogeneity in the distribution of Sr atoms. In fact the susceptibility curve for polycrystalline Y124 with 30% Sr is relatively broad, which indicates some disorder or nonhomogeneity. In general T_c of Y124 single crystals is slightly lower than in polycrystalline samples of the same composition. This problem has been investigated in the past.[21] Single-crystal x-ray refinement shows that the occupation of the Cu2 site can be slightly lower than 100% due to some substitution from crucible material, which can contain impurities leading to a lowering of T_c.

B. Structural characterization of the single crystals

The results of the structural refinement of the crystals with different Sr content are presented in Table I–IV. Figure 3(a) displays the variation of the unit-cell volume as a function of Sr concentration. Lattice parameters decrease linearly with increasing Sr content due to the difference in ionic radii of Ba (1.52 Å) and Sr (1.36 Å).[6] The changes of lattice constants as well as of other important structural parameters for a given Sr content interval Δx normalized to the value at $x=0$ are presented in Table IV. The extent of the lattice shrinkage was evaluated to be 2.7%, 0.9%, and 2.2% per Sr atom per formula unit for the crystallographic *a*, *b*, and *c* axis, respectively. The shrinkage of the *b* axis is less pronounced than the reduction of the *a* and *c* axis. This can be explained taking into account the fact that the double-chain structure (*b* axis direction) is the most rigid part of the Y124 lattice. The different extents of contraction in the lattice dimensions of the $Y(Ba_{1-x}Sr_x)_2Cu_4O_8$ phases indicate that the effect of chemical pressure resulting from the substitution of Sr for Ba is rather anisotropic. This finding is in an accordance with the data on the Y247 system[25] and contradicts the behavior observed in the Sr-doped Y123 system.[26] In the latter case, the shrinkage of the lattice parameters was found to be almost isotropic. The strain, or orthorhombic distortion, defined as $S=2(b-a)/(b+a)$ increases with increasing Sr content [Fig. 3(b)], which is similar to the trend observed in the Sr-substituted Y247 system[25] and powder Sr-substituted Y124 samples.[17,18] On the other hand, this is in contrast to the behavior reported on $Y(Ba_{1-x}Sr_x)_2Cu_3O_w$,[26] where *S* was found to be a nonmonotonic function of *x*.

The buckling of the CuO_2 planes does not exhibit a considerable variation as a function of *x*. The values of the Cu2-O2-Cu2 and Cu2-O3-Cu2 angles are about the same, both being around 165°.

From the data presented in Table IV and a comparison with the values corresponding to pressure-induced changes in the Y124 structure[27] some interesting observations can be drawn: Substitution of 30% Ba with Sr is equivalent to the application of an external pressure of about 2.2 GPa. A complete substitution ($x=1$) would induce a change of the parameters equivalent to the application of about 9.3 GPa external pressure.

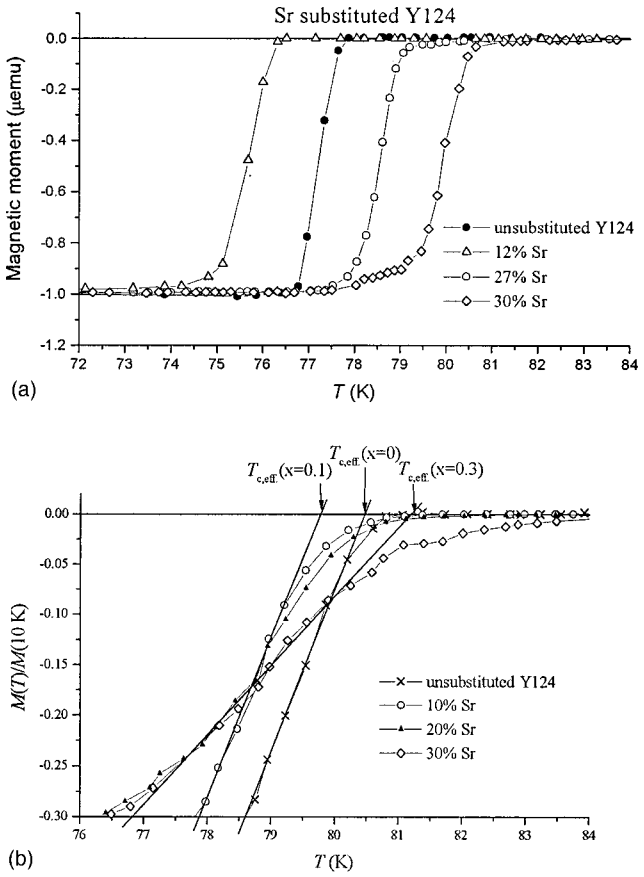

FIG. 2. Magnetization of $Y(Ba_{1-x}Sr_x)_2Cu_4O_8$ (a) single crystals and (b) powder with various Sr content.

Figure 4 shows the fractional change of different bond lengths as a function of Sr content. The biggest change occurs for the Cu2-O1 bond. Also noticeable changes are found for the Ba-O4 and the Cu2-O2 bonds.

An important modification of the structure is the decrease of the thickness of the charge reservoir (Fig. 5), defined as the part of the unit cell between the weighted CuO_2 planes, including the CuO chains and the Ba/Sr atoms. With increasing Sr content, the superconducting blocks are coming closer, which leads to a better coupling. One can therefore expect a lower anisotropy γ of the crystals. In fact investigations of superconducting parameters show a decrease of γ from 12 for nonsubstituted Y124 to 9 for Sr-substituted Y124 crystals.[20]

The distance between CuO_2 planes increases as a function of Sr content, hence the thickness of the superconducting block (the Cu2-Cu2 distance) increases.

IV. THE INFLUENCE OF Sr SUBSTITUTION ON CHARGE DISTRIBUTION IN THE STRUCTURE FROM BVS CALCULATION

A very useful method for the determination of charge distribution in the structure is the concept of BVS, which was developed by Brown and Altermatt.[28] The BVS method was successfully applied for various compounds by Cava *et al.*[29] Tallon,[15] and Karppinen and Yamauchi.[30] Using this method it is possible to describe the distribution of holes between various structural elements like the CuO_2 planes in the infinite-layer block and the charge-reservoir block.

The bond-valence sum s_{ij} of bonds between atoms (or ions) i and j in a solid matrix is calculated from experimental bond lengths r_{ij} (in Å) as

$$V_i = \pm \sum s_{ij} = \pm \sum \exp[(R_{ij}^0 - r_{ij})/0.37], \qquad (1)$$

where R_{ij}^0 (in Å) is an empirically determined parameter, specific for each different *i-j* pair of ion atoms.[28] Positive values are given for metal atoms and negative values for the oxygen atoms.

According to Brown,[31] using Eq. (1) it is possible to determine the distribution of charge between Cu atoms after applying three corrections.

(1) The parameters R_o have been determined at room temperature. Bond length determined at other temperatures must be corrected to room temperature.

(2) The values of R_o depend on the oxidation state. For Cu valence between 2 and 3 (or 1 and 2) one has to use corrections. For the calculation of the average valence of copper (for the case of the valence between 2 and 3) one has to use the equation

$$y = (V_2 - 2)/(V_2 + 1 - V_3), \qquad (2)$$

where y is the fraction of Cu^{+3} and $(1-y)$ the fraction of Cu^{+2}. Parameter V_2 is the BVS of copper calculated using $R_o(Cu^{+2})$, V_3 is the BVS of copper calculated using $R_o(Cu^{+3})$. The valence of Cu is thus

TABLE IV. Compressibility of lattice parameters and bonds in the family of $Y_2(Ba_{1-x}Sr_x)_4Cu_nO_{2n+\delta}$ compounds as a function of Sr content x. d(Cu2-O1), distance between Cu2 and O1 atoms.

Parameter	Y124 present work	Y124 powder (Ref. 17)	Y123 (Ref. 26)	Y247 (Ref. 25)
$(\Delta a/\Delta x)/a_0$	-27.6×10^{-3}	-24.1×10^{-3}	-19.6×10^{-3}	-28×10^{-3}
$(\Delta b/\Delta x)/b_0$	-9.2×10^{-3}	-10.3×10^{-3}	-17.5×10^{-3}	-14×10^{-3}
$(\Delta c/\Delta x)/c_0$	-21.6×10^{-3}	-18.6×10^{-3}	-20.2×10^{-3}	-33.9×10^{-3}
$(\Delta V/\Delta x)/V_0$	-58.1×10^{-3}	-52.7×10^{-3}	-56.8×10^{-3}	-72.6×10^{-3}
$[\Delta$(Cu2-O1)$/\Delta x]/d$(Cu2-O1)	-57.7×10^{-3}		-60.8×10^{-3}	
$[\Delta$(Cu2-Cu2)$/\Delta x]/d$(Cu2-Cu2)	$+21.1\times10^{-3}$		$+27.9\times10^{-3}$	
$[\Delta$(Ba-O4)$/\Delta x]/d$(Ba-O4)	-31.1×10^{-3}			

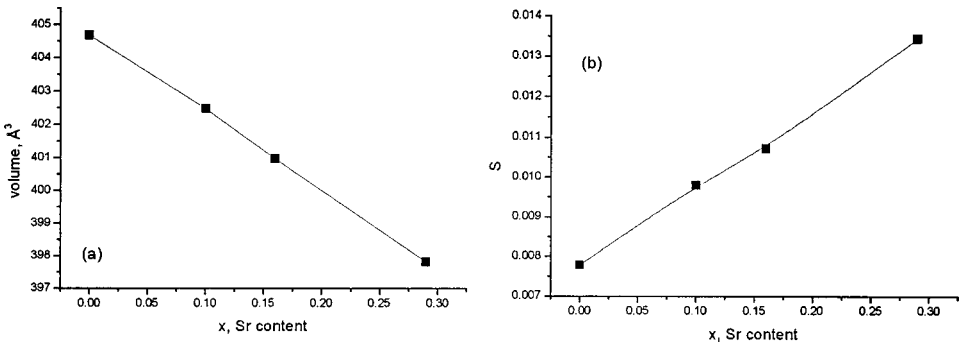

FIG. 3. (a) Variation of the unit-cell volume of $Y(Ba_{1-x}Sr_x)_2Cu_4O_8$ crystals as a function of Sr concentration, (b) strain, or orthorhombic distortion, defined as $S=2(b-a)/(b+a)$ as a function of Sr content in $Y(Ba_{1-x}Sr_x)_2Cu_4O_8$.

$$V=3y+2(1-y)=2+y=(3V_2-2V_3)/(V_2+1-V_3). \quad (3)$$

The values V(Cu1) and V(Cu2) calculated in this way are shown in the Table III. Both valences V(Cu1) and V(Cu2) increase with Sr content, which is in disagreement with the NQR data, which show an increase of hole number in Cu2, while the hole number in Cu1 decreases. The reason of this discrepancy can be strain in the lattice.

(3) Correction of the BVS of copper for the strain.

If the bonds length are strained they will not correlate properly with the bond valence. A procedure proposed by Brown[31] is as follows: After calculating the average BVS of Cu using corrections (1) and (2) one has to calculate the average BVS of Cu from the stoichiometry for a given compound. This is 2.25 for Y124. If this value differs from the average BVS Cu calculated from structural data, one should add (subtract) the difference to each BVS of Cu. This is with the assumption that the influence of stress is equal on all Cu sites. The result is shown in the Table V and Fig. 6 as V(Cu1,2) true value. One can see that after correction, the BVS of Cu1 decreases and the BVS of Cu2 increases with Sr content by the same value, which is in agreement with NQR data.

The holes, which are responsible for superconductivity, may be placed either on Cu or on O atoms in the CuO_2 planes. The importance of the hole distribution between Cu and O sites within the CuO_2 planes was suggested by several authors using NQR investigations[12,13] as well as BVS analysis.[15]

The NQR analysis of Zheng *et al.*,[12] showed that ratio of number of holes on copper to number of holes on oxygen in planes n(Cu)/2n(O) increases from $YBa_2Cu_3O_7$ to $YBa_2Cu_4O_8$. Simultaneously T_c decreases. In order to increase T_c significantly, the number of holes on both copper and oxygen in planes has to increase. In fact, NQR investigation of Y124 (Zheng *et al.*[13]) leads to the conclusion that at high hydrostatic pressure the number of holes on both Cu and O sites increases without changing the n(Cu)/2n(O) ratio causing a larger increase of T_c.

In order to investigate the distribution of holes between copper and oxygen as a function of Sr content we have calculated the BVS of all four oxygen atoms using a weighted value of the $R_o(Cu^{Vtrue}\text{-}O^{-2})$ parameter, where Vtrue is the V(Cu1,2) value (Table V) after the correction for stress. The result shows that the BVS of O1 (apical oxygen) increases, the BVS of plane oxygen atoms O2,3 decreases, while the BVS of chain O4 oxygen does not change. This indicates a redistribution of the charge between copper and oxygen atoms with Sr substitution. The BVS of O1 increases from -2.044 to -1.985 indicating a charge transfer from Cu1 to O1. The BVS of O2 decreases from -2.054 to -2.087 and the BVS of O3 decreases from -2.045 to -2.069, indicating a charge transfer from O2 and O3 to Cu2.

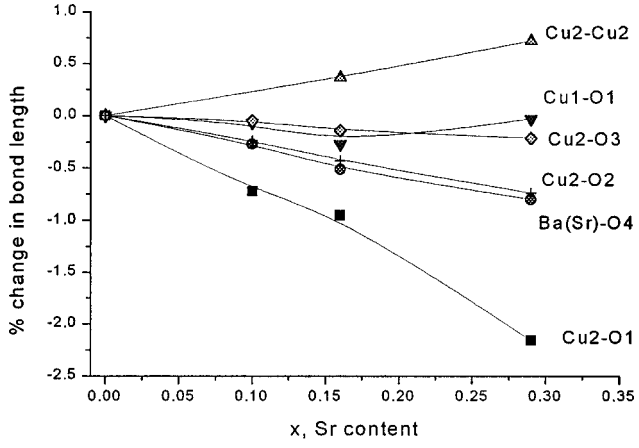

FIG. 4. Change of different bond lengths as a function of Sr content in $Y(Ba_{1-x}Sr_x)_2Cu_4O_8$ crystals.

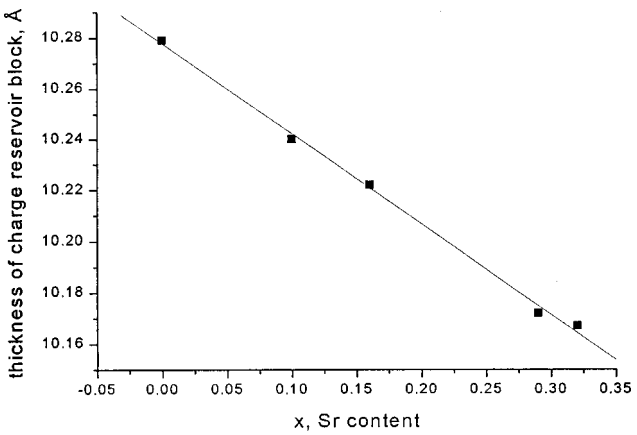

FIG. 5. Charge-reservoir thickness in the $Y(Ba_{1-x}Sr_x)_2Cu_4O_8$ crystals as a function of Sr content.

TABLE V. Bond valence sums (BVS's) of copper and oxygen in $Y(Ba_{1-x}Sr_x)_2Cu_4O_8$. V_2Cu1,2, BVS of Cu1,2 calculated with $R_o(Cu^{+2}\text{-}O^2)$; V_3Cu1,2, BVS of Cu1,2 calculated with $R_o(Cu^{+3}\text{-}O^2)$. VCu1,2, BVS of Cu1,2 calculated from the form (3); VCu(average)=(VCu1+VCu2)/2; VCu1,2 true, VCu1,2+strain correction; BVS $O_i/R_o(Cu^{Vtrue}\text{-}O^2)$, BVS of oxygen calculated with VCu1,2 true; BVS/$R_o(Cu^{+2.25}\text{-}O^2)$, BVS of oxygen calculated with VCu$^{+2.25}$; V(plane), number of holes in the CuO_2 plane calculated from Eq. No. (4).

X, Sr	V_2Cu2	V_3Cu2	V_2Cu2	V_2Cu1	V_3Cu1	VCu1	VCu (average)	Strain correction	VCu2true	VCu1true
0	2.150	2.468	2.220	2.218	2.546	2.324	2.272	−0.022	2.198	2.302
0.11	2.175	2.497	2.258	2.223	2.551	2.332	2.295	−0.045	2.213	2.287
0.16	2.192	2.516	2.285	2.231	2.560	2.344	2.315	−0.0645	2.221	2.280
0.31	2.230	2.559	2.342	2.236	2.566	2.352	2.347	−0.097	2.245	2.255

	BVS O1		BVS O2		BVS O3		BVS O4		V plane
	$R_o(Cu^{Vtrue}\text{-}O^{-2})$	$R_o(Cu^{+2.25}\text{-}O^{-2})$	$R_o(Cu^{Vtrue}\text{-}O^{-2})$	$R_o(Cu^{+2.25}\text{-}O^{-2})$	$R_o(Cu^{Vtrue}\text{-}O^{-2})$	$R_o(Cu^{+2.25}\text{-}O^{-2})$	$R_o(Cu^{Vtrue}\text{-}O^{-2})$	$R_o(Cu^{+2.25}\text{-}O^{-2})$	
0	2.044	2.039	2.054	2.059	2.045	2.051	1.953	1.938	0.099
0.11	2.022	2.013	2.062	2.064	2.050	2.052	1.952	1.939	0.101
0.16	2.020	2.003	2.071	2.070	2.058	2.057	1.952	1.938	0.092
0.31	1.985	1.962	2.087	2.081	2.069	2.062	1.948	1.938	0.089

The introduction of the stress correction only for Cu can raise a question about the necessity of additional stress corrections for oxygen. The average BVS of oxygen is 2.023 ±0.002 and has the same value for all measured crystals independently of Sr content. Stress created by Sr substitution does not influence the average BVS of oxygen calculated in that way.

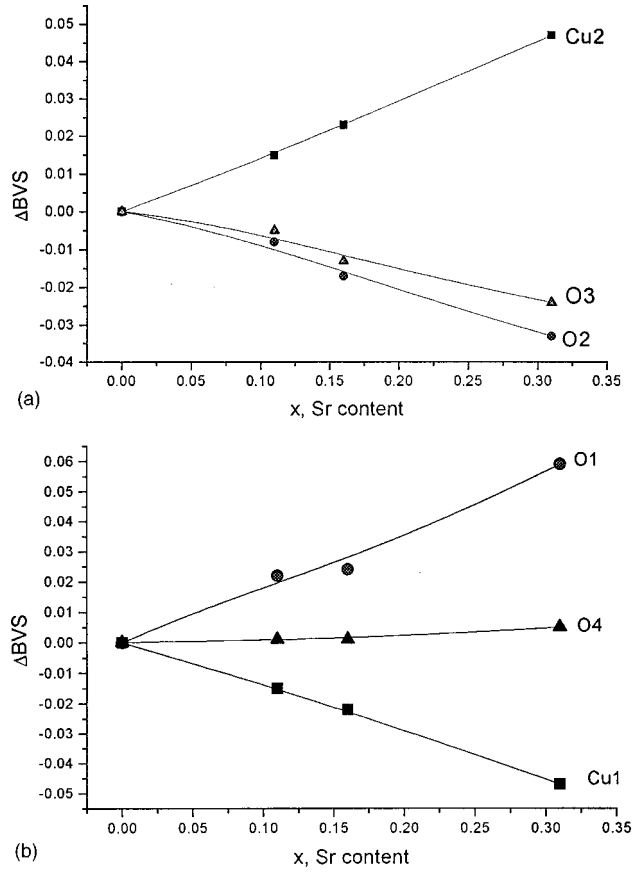

FIG. 6. Change of the BVS (Δs) of copper and oxygen as a function of Sr content in $Y(Ba_{1-x}Sr_x)_2Cu_4O_8$ crystals. (a) BVS of plane Cu2 and O2,3, (b) BVS of chain Cu1 and O1,4.

Using these data we can calculate the total number of holes in the plane. Let us assume that number of holes in copper in plane is $n(\text{Cu2})=V(\text{Cu2})-2$ and number of holes in oxygen in plane is: $n(\text{O2,3})=-V(\text{O2,3})+2$. Figure 6 shows the change of the number of holes per atom as a function of Sr content. Total number of holes in the plane is

$$V(\text{plane})=n(\text{Cu2})+n(\text{O2})+n(\text{O3}) = V(\text{Cu2})-V(\text{O2})-V(\text{O3})+2. \quad (4)$$

The result is shown in Table V. In this model charge in the plane and in the chain remains almost constant and only redistribution of charge between copper and oxygen within the plane and the chain occurs. The strain correction has a significant influence on the final result. Without strain correction the increase of the BVS of Cu2 is larger: $\Delta V(\text{Cu2})=0.122$ hole per copper for $\Delta x=0.3$ (instead of 0.047) and the total charge in the planes increases by $\Delta V(\text{plane})=0.089$ hole if we calculate BVS O2,3 using $R_o(Cu^{+2.25}\text{-}O^{-2})$. This seems to be nonrealistic.

Hence, there are two macroscopic parameters important for T_c: the total number of holes in the CuO_2 planes and the distribution of holes between oxygen and copper sites. For a fixed number of holes in CuO_2 planes, T_c increases with a preferential hole distribution on oxygen sites.

In the case of Sr substitution in Y124, the total number of holes in the plane seems to be constant. Substitution of Sr for Ba increases number of holes in plane copper Cu2, but decreases the number of holes located in plane oxygen O2,3. Finally, T_c increases only by 2–3 K. If we are able to shift more holes from copper to oxygen, T_c could rise more.

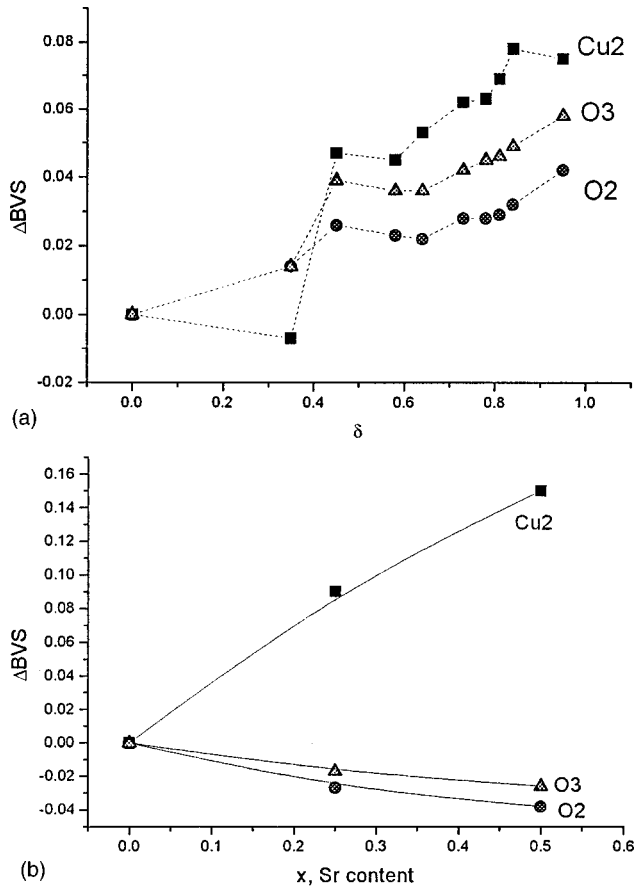

FIG. 7. (a) Change of BVS of plane atoms in $YBa_2Cu_3O_{6+\delta}$ as a function of oxygen content. Structural data from Cava *et al.* (Ref. 29). (b) Change of BVS of plane atoms in $Y(Ba_{1-x}Sr_x)_2Cu_3O_{6+\delta}$ as a function of Sr content. Structural data from Licci *et al.* (Ref. 26).

V. THE EFFECT OF DIFFERENT DISTRIBUTION OF HOLES IN CuO_2 PLANES AS A FUNCTION OF OXYGEN AND STRONTIUM DOPING IN Y123

The importance of the hole distribution within the planes, not only the total number of holes, can be shown in the example of Y123:Sr compound. Using data of Cava *et al.*[29] and Licci *et al.*[26] we have calculated the change in BVS of Cu2, O2, and O3 as a function of Sr and O content. Figure 7(a) shows the ΔS as a function of oxygen content δ in $YBa_2Cu_3O_{6+\delta}$. All BVS's increase with oxygen content, showing a well-known two-plateau dependence similar to T_c behavior. The hole concentration on Cu2 and O^{2}_{3} increases with oxygen doping.

The distribution of holes is very different after the substitution of Sr. Figure 7(b) shows ΔS of Cu2, O2, and O3 as a function of Sr content. We did not introduce corrections for the stress in the Licci *et al.*[26] data. The BVS of Cu2 increases, but the BVS of the plane oxygen atoms decreases. This is similar to Y124:Sr as shown before. A significant change of the charge distribution in the CuO_2 planes takes place. The difference in the BVS of plane Cu and O atoms is related to the different dependence of the out-plane bond length Cu2-O1, O2,3-Ba/Sr, and O2,3-Y as a function of doping with O and Sr. An increase of the oxygen content causes a nearing of CuO_2 planes and shortening of these bonds. For all plane Cu and O atoms, the BVS increases. With increasing Sr content the CuO_2 planes are going apart and the O2,3-Y bond increases. This structural difference is connected with the change of the hole distribution in the CuO_2 planes. Hence, the BVS increases for Cu2, but decreases for O2,3 and consequently more holes are located on Cu2.

VI. COMPARISON OF THE PRESSURE EFFECT AND Sr SUBSTITUTION ON THE STRUCTURE, BVS, AND T_c IN Y124 AND Y123

The variation of the structure of the compounds Y123 and Y124 as a function of Sr substitution is very similar, but the T_c behavior is different. With increasing Sr content T_c decreases in Y123,[26,32] but slightly increases in Y124. As both compounds have a positive T_c dependence on pressure, we can try to find differences by a comparison of pressure and substitution effects on the structures of both compounds. In the case of underdoped Y123 crystals $dT_c/dp = 4-6$ K/GPa. Optimally doped material has dT_c/dp close to zero. As discussed by Marezio, Licci and Gauzzi[32] the application of pressure on Y123 in comparison to the substitution of Sr for Ba leads to the following structural changes.

(1) Chemical pressure leads to an almost isotropic contraction of all three lattice parameters. The contraction of the *c* axis at high pressure is more than twice of those observed along the other two axes.

(2) The thickness of the superconducting block, the Cu2-Cu2 distance, increases with Sr substitution and decreases with pressure. In this case the effect of Sr substitution and pressure are opposite.

(3) The complete substitution of Sr for Ba would induce a variation of the lattice parameters equivalent to an external pressure of about 1 GPa.

(4) The apical bond length Cu2-O1 decreases with both substitution of Sr for Ba and pressure.

For Y124 T_c increases with pressure: $dT_c/dp = 5.5$ K/GPa. The application of pressure on Y124 in comparison to the substitution of Sr for Ba leads to the following structural changes.

(1) Chemical pressure leads to an anisotropic contraction of lattice parameters: the contraction in *b* direction is three times smaller than the contraction in *a* and *c* directions. From the data of Nelmes *et al.*[27] the compressibility in *b* direction is 3.5–4 times smaller than that in *a* and *c* direction.

(2) The thickness of the superconducting block (the Cu2-Cu2 distance) increases with Sr substitution and decreases with pressure. In this case the effect of Sr substitution and pressure are opposite.

(3) The substitution of 0.3 Sr for Ba induces a variation of the lattice parameters equivalent to an external pressure of 2.2 GPa.

(4) The apical bond length Cu2-O1 decreases with substitution of Sr for Ba and pressure.

Both Sr substitution and high pressure lead to an increase of the hole concentration in Cu in the planes. However, the distribution of holes between copper and oxygen is different.

The most important difference between the application of hydrostatic and chemical pressure in both Y123 and Y124 compounds is the behavior of the superconducting block. The distance between CuO_2 planes decreases with hydrostatic pressure. This brings Y atoms nearer to plane oxygen and increases the BVS of O2 and O3. Chemical pressure, on the other hand, increases the thickness of the superconducting block, and the distance between Y and CuO_2 plane. Therefore, the BVS of O2 and O3 decreases. Both chemical and hydrostatic pressure cause a contraction of the apical bond Cu2-O1 and an increase of the BVS of Cu2. Therefore, there is a significant difference in the hole distribution within the planes between Sr-substituted crystals and crystals under high pressure. From our BVS calculations presented in this work, we concluded that with Sr substitution the number of holes in Cu2 and O1 increases. Due to the lack of data on the R_o dependence on pressure we cannot make similar calculations for high pressure. The NQR investigation of Zheng *et al.*[13] show that the $n(\mathrm{Cu})/2n(\mathrm{O})$ parameter of Y124 does not change with pressure, although $n(\mathrm{Cu})+2n(\mathrm{O})$ increases, where $n(\mathrm{Cu})$ is the number of holes in Cu in planes and $n(\mathrm{O})$ is the number of holes in oxygen in planes.

The main structural difference between Y123 and Y124 behavior is the stiffness of the *b* axis in Y124 caused by the presence of double CuO chains.

Meingast *et al.*[33] investigated the uniaxial pressure dependence of T_c of Y123 and Y124 single crystals. They showed that the strong change of T_c in Y124 by pressure ($dT_c/dp = 5.5$ K/GPa) is caused mainly by the *a*-axis contribution, whereas due to the low compressibility in the *b* direction the *b*-axis contribution is small. The experimental dT_c/dp_i values are $dT_c/dp_a = +(3.7-5.0)$ K/GPa, $dT_c/dp_b = +(0.3-0.4)$ K/GPa, and $dT_c/dp_c = (0\pm0.7)$ K/GPa.[33]

The behavior of Y123 is different. For optimally doped Y123 material $dT_c/dp \approx 0$, but there are quite large dT_c/dp_i values occurring for uniaxial pressure within the (*a*,*b*) plane [$dT_c/dp_a = +(2-3)$ K/GPa, $dT_c/dp_b = -(2-3)$ K/GPa], which in case of a hydrostatic pressure cancel each other due to their opposite signs. However, since Y124 is underdoped it should be compared with underdoped Y123. For underdoped Y123 crystals under hydrostatic pressure $dT_c/dp = 4-6$ K/GPa, which results from high uniaxial pressure effect along *c* axis. The dT_c/dp_a and dT_c/dp_b are nearly doping independent. Both Y123 (underdoped) and Y124 have a large positive hydrostatic pressure effect on T_c, however their uniaxial values are quite different. The large dT_c/dp is caused in underdoped Y123 by uniaxial pressure effect along the *c* axis and in Y124 by uniaxial pressure effect along the *a* axis.

The differences in the uniaxial pressure dependence can partially explain the different behavior of T_c in Y123 and Y124 with Sr substitution. Sr substitution in Y123 causes an isotropic contraction, so contributions from *a* and *b* axes cancel due to opposite signs. The Sr-induced *c*-axis contribution is much smaller than the one due to hydrostatic pressure.

For Y124 the substitution of Sr causes a compression of the *a* axis, which is similar to the pressure effect. For instance, substitution of $x=0.3$ Sr for Ba leads to a structural effect that is equivalent to an application of about 2.2 GPa hydrostatic pressure. As for Y124 $dT_c/dp = 5.5$ K/GPa, consequently one expects an increase of T_c by about 12 K. Instead, we observe an increase of only 2–3 K. The reason of this is probably the increase of the thickness of the superconducting block with Sr substitution. Therefore the BVS of O2 and O3 decreases and T_c increases only a little bit.

A second reason why, despite of the increase of charge on Cu2 by Sr substitution, T_c does not increase as much as at high hydrostatic pressure, could be the introduction of disorder in the structure through partial Sr substitution. The NQR experiments show that Sr substitution dramatically increases the NQR linewidth, which is a clear indication of an increased lattice disorder. This additional disorder presumably attenuates the increase of T_c with Sr content. As shown by Attfield, Kharlanov, and McAllister[24] disorder leads to a decrease of T_c in the Ln-214. We have investigated the influence of disorder in RE124 (Ref. 34) and found that T_c decreases with the disorder parameter.

VII. NQR MEASUREMENTS ON $Y(Ba, Sr)_2Cu_4O_8$ POWDER SAMPLES

It is very important to use an independent method, which can prove the variations of hole concentration in Cu1 and Cu2 by substitution of Sr for Ba. The NQR frequency ν_Q of the plane copper is very sensitive to changes in the density of hole charge carriers *n* in the CuO_2 planes. The NQR experiments for $YBa_2Cu_3O_{7-x}$ and $La_{2-x}Sr_xCuO_4$ show that ν_Q of the plane copper nuclei shifts towards higher values with increasing *n*. In the $YBa_2Cu_3O_{7-x}$ family ν_Q changes at 100 K from 23.18 MHz in underdoped $YBa_2Cu_3O_6$ to 31.53 MHz in $YBa_2Cu_3O_7$. In the $La_{1-x}Sr_xCuO_4$ system, ν_Q increases linearly upon Sr doping from 33 MHz for $x=0$ to 36.2 MHz for $x=0.15$. With the assumption that each Sr ion delivers a hole charge carrier in Cu2 one gets a change $d\nu_Q/dn \approx 21$ MHz/hole. This result we can use to estimate the increase of *n* in Cu2 of $YBa_{2-x}Sr_xCu_4O_8$ when Ba is substituted through isovalent Sr. The measurements of ν_Q of plane copper in $YBa_{2-x}Sr_xCu_4O_8$ show that ν_Q increases by 330 kHz for $x=0.3$ and by 610 kHz for $x=0.6$ as compared to ν_Q for pure $x=0$ material. As one can notice the increase in ν_Q is approximately linear in *x* (see Table VI). Now, assuming the relation $d\nu_Q/dn \approx 21$ MHz/hole also holds in the case of Sr for Ba substitution in $YBa_2Cu_4O_8$, one can conclude that the hole-charge carrier concentration in Cu2 increased by 0.016 hole/Cu for $x=0.3$ and 0.029 hole/Cu for $x=0.6$. Since Sr and Ba are isovalent, this increase has to come from a charge redistribution in the structure. The ν_Q of the chain copper decreases with *x* for almost the same value as the ν_Q of plane copper increases. Simultaneously the BVS of O1 increases and the BVS of O2,3 decreases. This is a clear indication that a transfer of holes between copper and oxygen is taking place. The calculated charge transfer differs when BVS and NQR results are used. This is understandable since both methods can still be influenced by other effects like volume change by substitutions, strain, etc.

TABLE VI. NQR frequencies and linewidth of plane and chain ^{63}Cu in pure and Sr-substituted $YBa_2Cu_2O_8$ (Y124).

	NQR freq. of plane copper $^{63}\nu_Q$(Cu2) (MHz)	Linewidth $\Delta^{63}\nu_Q$(Cu2) (kHz)	NQR freq. of chain copper $^{63}\nu_Q$(Cu1) (MHz)	Linewidth $\Delta^{63}\nu_Q$(Cu1) (kHz)	Difference between $^{63}\nu_Q$(Cu2) in Sr doped and pure Y124 (kHz)	Difference between $^{63}\nu_Q$(Cu1) in Sr doped and pure Y124 (kHz)	Charge transfer (holes per copper)
$YBa_2Cu_4O_8$	29.770	150	20.005	56	0	0	0
$YBa_{1.7}Sr_{0.3}Cu_4O_8$	30.100	1140	19.660	640	330	−345	0.016
$YBa_{1.4}Sr_{0.6}Cu_4O_8$	30.380	1350	19.375	840	610	−630	0.029

VIII. CONCLUSIONS

The influence of substitution of Sr for Ba in the Y124 compound on the structure, charge distribution, and T_c has been investigated and compared with the literature data for Y123 and hydrostatic-pressure effect on both compounds.

(1) The substitution of Sr for Ba in Y124 and Y123 induces a variation of the structural parameters causing charge redistribution. In the planes, holes from O2,3 atoms transfer to Cu2 and in the chain, holes from Cu1 transfer to O1 (apical) atom.

(2) The transition temperature slightly increases with Sr content in Y124, but less than expected from the increase of the number of holes in Cu2. In Y123 T_c decreases upon Sr substitution.

(3) Chemical pressure leads to an anisotropic contraction of lattice parameters in Y124: the contraction in *b* direction is three times smaller than in *a* and *c* directions. This is the main difference between Y124 and Y123. In Y123 chemical pressure leads to an isotropic contraction of lattice parameters.

(4) At high hydrostatic pressure, T_c of Y124 increases due to a contraction of the *a* axis with pressure and Sr substitution leads also to the contraction of the *a* axis. In Y123 the contraction of all axes is isotropic with Sr substitution, but the contraction of the *c* axis at high pressure is more than twice the amount of those observed along the other two axes. This can explain why T_c increases slightly for Y124 with Sr substitution, but decreases for Y123.

(5) The apical bond length Cu2-O1 decreases with substitution of Sr for Ba, which causes an increase of the BVS and hole number in Cu2 in both Y124 and Y123.

(6) The thickness of the superconducting block increases and the thickness of charge reservoir decreases with Sr substitution in both Y124 and Y123, which causes a shift of holes from oxygen to copper in the planes.

ACKNOWLEDGMENTS

This work has been supported by the Swiss Science National Foundation and INTAS project.

*Corresponding author. FAX: +4116331072. Email address: karpinski@solid.phys.ethz.ch

[1] J. Karpinski, E. Kaldis, E. Jilek, S. Rusiecki, and B. Bucher, Nature (London) **336**, 660 (1988).
[2] P. Bordet, C. Chaillout, J. Chenavas, J. L. Hodeau, M. Marezio, J. Karpinski, and E. Kaldis, Nature (London) **334**, 596 (1988).
[3] J. Hofer, J. Karpinski, M. Willemin, G. Meijer, E. Kopnin, R. Molinski, H. Schwer, C. Rossel, and H. Keller, Physica C **297**, 103 (1998).
[4] D. Zech, C. Rossel, L. Lesne, H. Keller, S. L. Lee, and J. Karpinski, Phys. Rev. B **54**, 12535 (1996).
[5] C. Rossel, J. Karpinski, and E. Kaldis, Physica B **194–196**, 2133 (1994).
[6] R. D. Shannon, Acta Crystallogr., Sect. A: Cryst. Phys., Diffr., Theor. Gen. Crystallogr. **A32**, 751 (1976).
[7] C. W. Chu, P. H. Horr, L. Gao, R. L. Meng, Z. J. Huang, and Y. Q. Wang, Phys. Rev. Lett. **58**, 405 (1987).
[8] R. J. Cava, R. B. van Dover, B. Batlogg, and E. A. Rietman, Phys. Rev. Lett. **58**, 408 (1987).
[9] T. Wada, S. Adachi, T. Mihara, and R. Inaba, Jpn. J. Appl. Phys., Part 2 **26**, L706 (1987).
[10] M. A. Subramian and M. H. Whangbo, J. Solid State Chem. **109**, 410 (1993).
[11] E. Kaldis, P. Fischer, A. W. Hewat, E. A. Hewat, J. Karpinski, and S. Rusiecki, Physica C **159**, 668 (1989).
[12] G. Zheng, Y. Kitaoka, K. Ishida, and K. Asayama, J. Phys. Soc. Jpn. **64**, 2524 (1995).
[13] G. Zheng, T. Mito, Y. Kitaoka, K. Asayama, and Y. Kodama, Physica C **243**, 337 (1995).
[14] M. Merz, N. Nücker, P. Schweiss, S. Schuppler, C. T. Chen, V. Chakarian, J. Freeland, Y. U. Idzerda, M. Kläser, G. Müller-Vogt, and Th. Wolf, Phys. Rev. Lett. **80**, 5192 (1998).
[15] J. Tallon, Physica C **168**, 85 (1990).
[16] B. Bucher, J. Karpinski, E. Kaldis, and P. Wachter, Physica C **157**, 478 (1989).
[17] T. Wada, T. Sakurai, N. Suzuki, S. Koriyama, H. Yamauchi, and S. Tanaka, Phys. Rev. B **41**, 11 209 (1990).
[18] T. Ishigaki, F. Izumi, T. Wada, N. Suzuki, Y. Yaegashi, H. Asano, H. Yamauchi, and S. Tanaka, Physica C **191**, 441 (1992).
[19] M. Van Bael, A. Kareiva, G. Vanhoyland, J. D'Haen, M. D'Olieslaeger, D. Franco, C. Quaeyhaegens, J. Yperman, J. Mullens, and L. Van Poucke, Physica C **307**, 209 (1998).
[20] M. Angst *et al.* (unpublished).
[21] J. Karpinski, G. I. Meijer, H. Schwer, R. Molinski, E. Kopnin, K. Conder, M. Angst, J. Jun, S. Kazakov, A. Wisniewski, R.

Puzniak, J. Hofer, V. Alyoshin, and A. Sin, Supercond. Sci. Technol. **12**, R153 (1999).
[22] V. Petricek and M. Dusek, JANA98 manual, 1998.
[23] J. Karpinski, E. Kaldis, S. Rusiecki, E. Jilek, P. Fischer, P. Bordet, C. Chaillout, J. Chenovas, J. L. Hodeau, and M. Maresio, J. Less-Common Met. **150**, 129 (1989).
[24] J. Attfield, A. Kharlanov, and J. McAllister, Nature (London) **394**, 157 (1998).
[25] T. R. Lu and Teng-Ming Chen, Physica C **276**, 75 (1997).
[26] F. Licci, A. Gauzzi, M. Marezio, G. P. Radaelli, R. Masini, and C. Chaillout-Bougerol, Phys. Rev. B **58**, 15 208 (1998).
[27] R. J. Nelmes, J. S. Loveday, E. Kaldis, and J. Karpinski, Physica C **172**, 311 (1990).
[28] I. D. Brown and D. Altermatt, Acta Crystallogr., Sect. B: Struct. Sci. **B41**, 244 (1985).
[29] R. Cava, A. Hewat, E. Hewat, B. Batlogg, M. Marezio, K. Rabe, J. Krajewski, W. Peck, and L. Rupp, Physica C **165**, 419 (1990).
[30] M. Karppinen and H. Yamauchi, Philos. Mag. B **79**, 343 (1999).
[31] I. D. Brown, J. Solid State Chem. **90**, 155 (1991).
[32] M. Marezio, F. Licci, and A. Gauzzi, Physica C **337**, 195 (2000).
[33] C. Meingast, J. Karpinski, E. Jilek, and E. Kaldis, Physica C **209**, 591 (1993).
[34] S. M. Kazakov *et al.* (unpublished).